Investigation of the defective structure in samples of a nickel heat-resistant alloy manufactured with a laser 3d printer

D. I. Davydov[1], A. A. Pilshchikov[2], N. I. Vinogradova[1], N. V. Kazantseva[1], E. V. Ezhov[1]

[1]Institute of Metal Physics, Ural Branch of the Russian Academy of Sciences, Ekaterinburg, Russia

[2]Snezhinsky Institute of Physics and Technology - branch of the Federal State Autonomous Educational Institution of Higher Professional Education "National Research Nuclear University "MEPHI", Snezhinsk, Russia

OUTLINE 1

The development of new heat-resistant nickel alloys for the creation of new generation aircraft products is included in the list of priority strategic directions of Russia.
Alloys of the Ni-Cr-Mo-Nb-Al system belong to the category of alloys with high heat resistance and structural stability. The main hardening phases in the dispersion-hardening KHN58MBYU (ХН58МБЮ) alloy are : γ′-фаза (Ni_3Al), niobium and chromium carbides containing molybdenum (MC, $M_{23}C_6$).
The mass content of the intermetallic γ′-phase (Ni_3Al) containing niobium in this alloy can reach 12%.
The alloy has good weldability and resistance to the formation of embrittling topologically close-packed (TCP) phases. However, uneven heating and stresses in the weld area contribute to a decrease in the service characteristics of the resulting part.

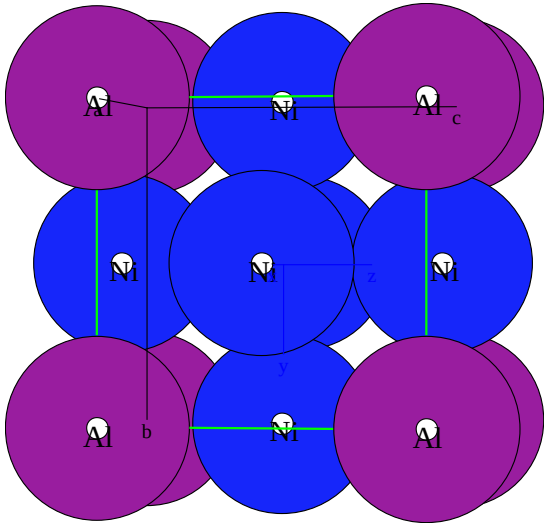

Ni_3Al-γ′ phase, $L1_2$, Cu_3Au-type, space group *Fm-3m*

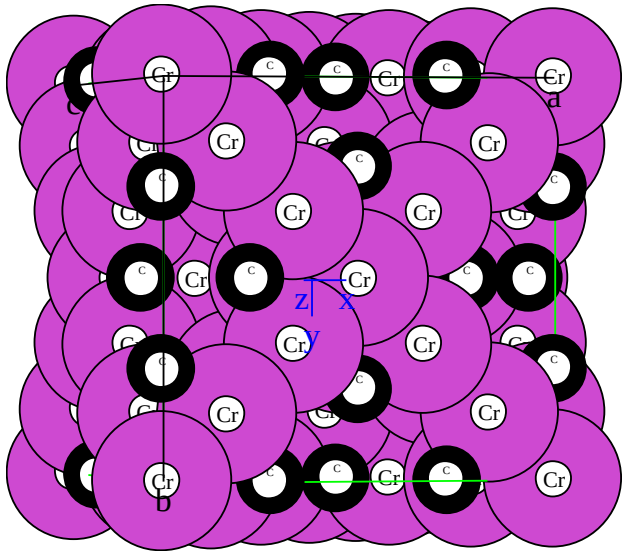

$Cr_{23}C_6$ carbide, B1, NaCl-type, space group *Fm3m*

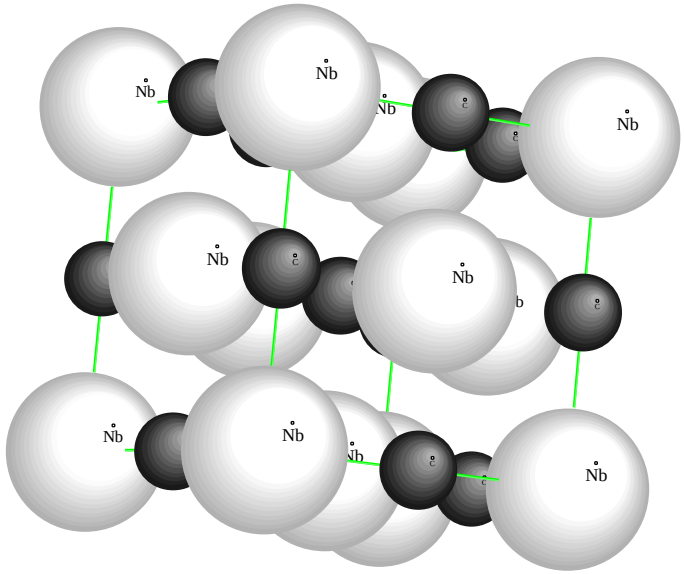

NbC carbide, B1, NaCl-type, space group *Fm-3m*,

OUTLINE 2

- Additive technology using 3D laser printing (L-PBF, laser powder-bed fusion) allows to obtain finished products of complex shape, eliminating the need for welding.
- Due to the high cooling rate and thermal cyclicity during printing in a 3D laser printer, the formation of nonequilibrium phases is possible in the structure of the obtained L-PBF sample, and there is also a high level of residual internal stresses, which manifests itself in the formation of nonequilibrium structures and internal defects.

- **In the presented report, the defects and features of the formation of equilibrium and nonequilibrium structures during 3D laser printing and subsequent heat treatment of the heat-resistant nickel alloy HN58MBYU used for the manufacture of gas turbine engine parts are considered.**

Работа выполнена по программе ИФМ УрО РАН "Аддитивность" 121102900049-1.

EXPERIMENTAL

- A spherical powder of the KHN58MBYU alloy was taken for the study. The chemical composition of the alloy according to GOST 5632-14 is shown in Table 1 (mass %).
- Alloy samples were obtained using a 3D laser printer Realizer SLM 100. The studies were performed on initial (L-PBF) samples and samples after annealing 800C-15h in an argon atmosphere.
- Structural studies were performed at the Center for Collective Use of the Institute of Metal Physics of the Ural Branch of the Russian Academy of Sciences using a scanning electron microscope JSM 6490 with energy dispersion and wave microanalysis Oxford Inca and transmission electron microscope Tecnai G2-30 Twin.
- X-ray phase analysis was performed using an X-ray diffractometer DRON-3, using Cu ka radiation.

Table 1. Chemical composition of the KHN58MBYU alloy

Ni	Cr	Mo	Fe	Al	Si	Ti	Nb
base	26-28	7-7.8	<3	1.25-1.55	<0.8	<0.2	2.7-3.4

RESULTS

X-ray analysis of the alloy samples (as-build and after aging 800C-15h)

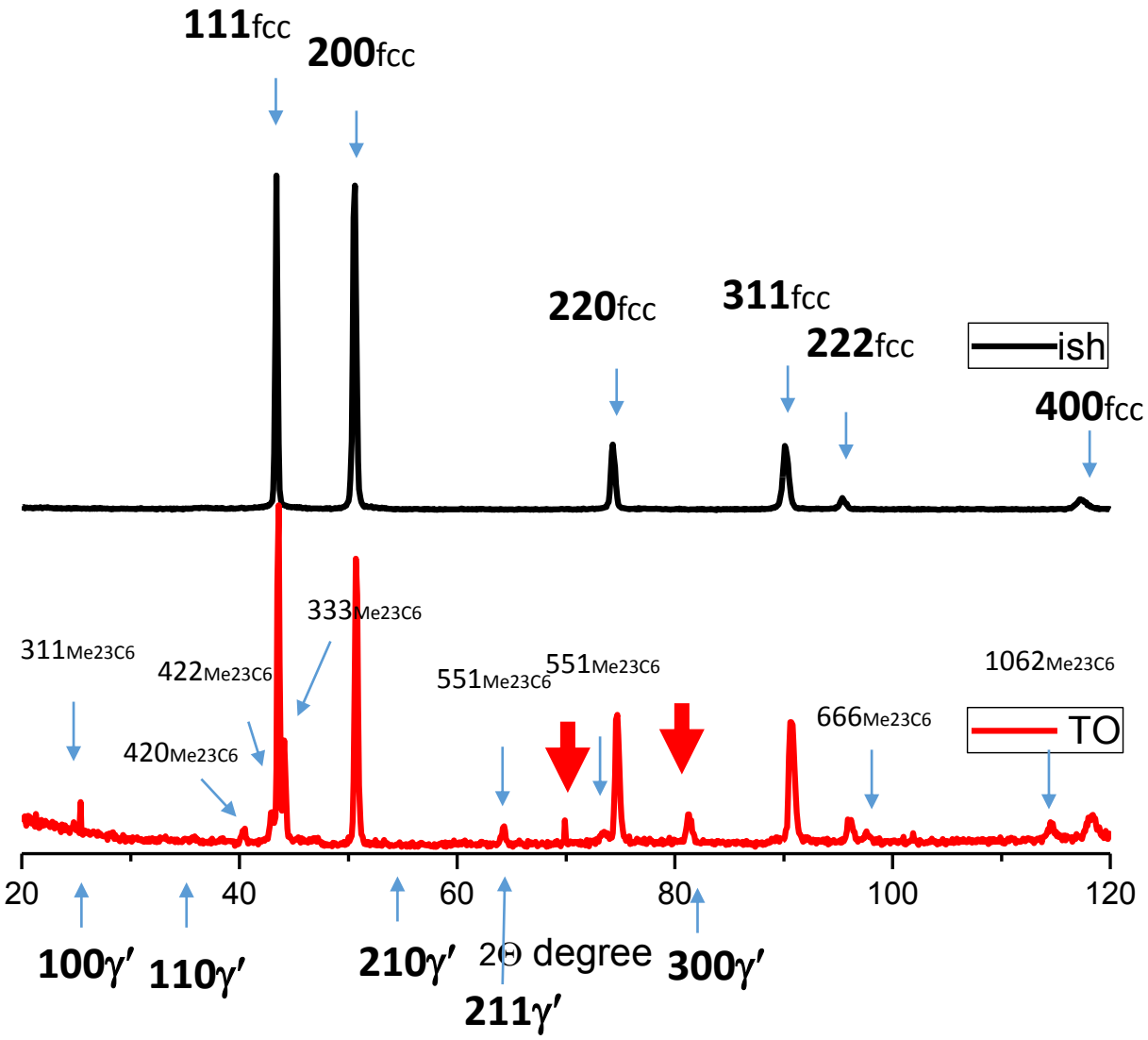

RESULTS

Structure of the alloy sample, as-build state, SEM

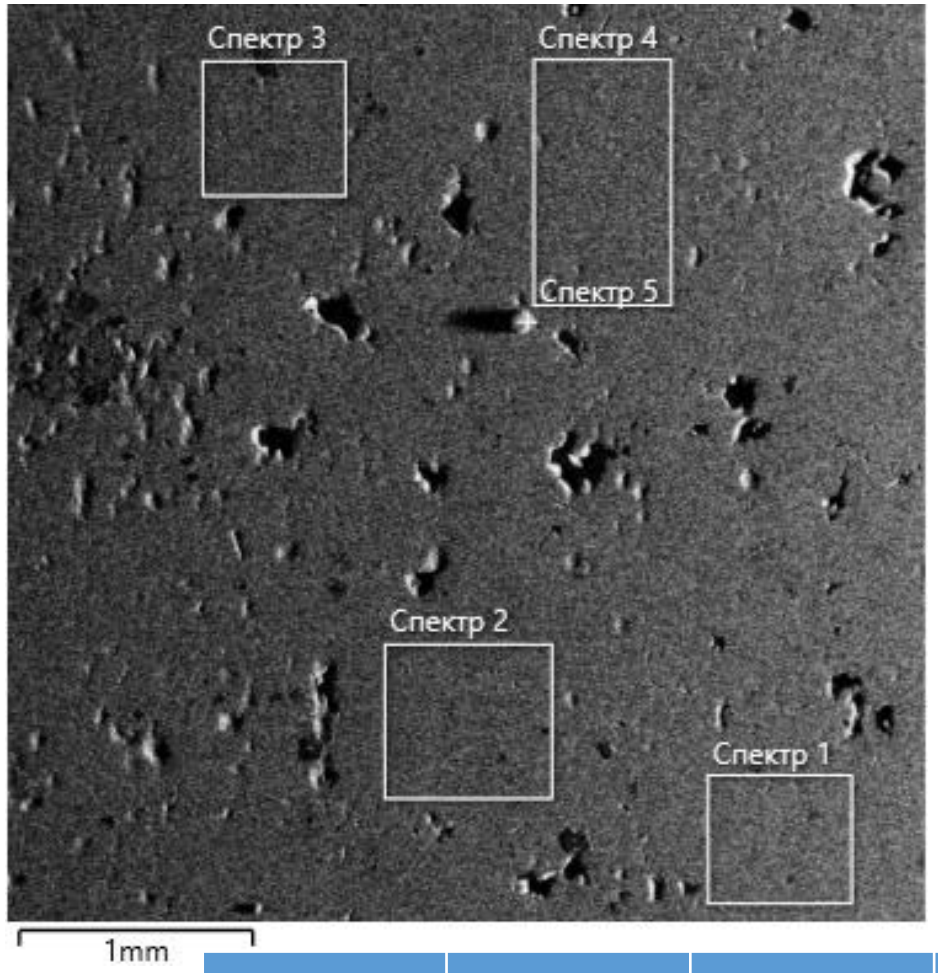

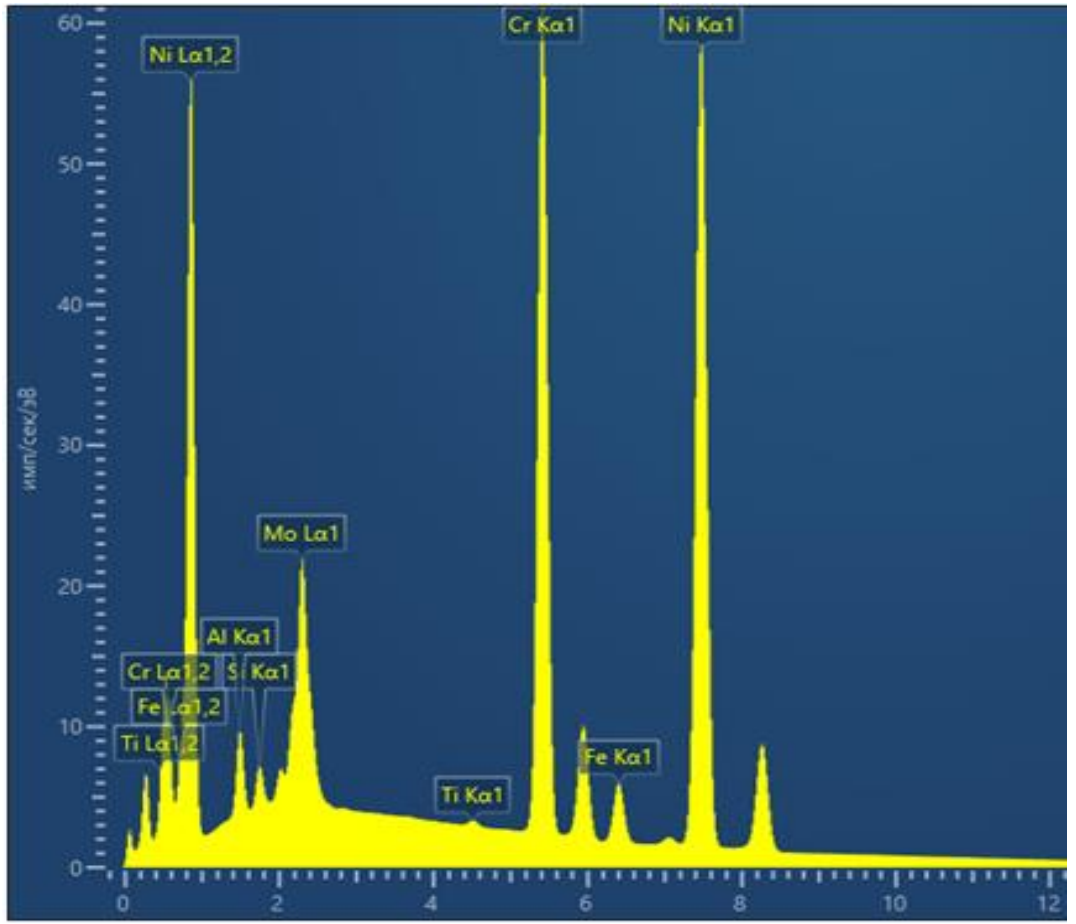

Ni	Cr	Mo	Fe	Al	Si	Ti
base	28.7	6.3	2.8	2.0	0.8	0.2

RESULTS

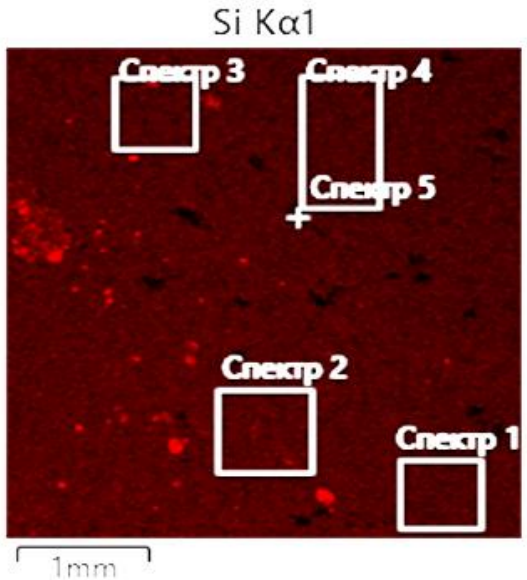

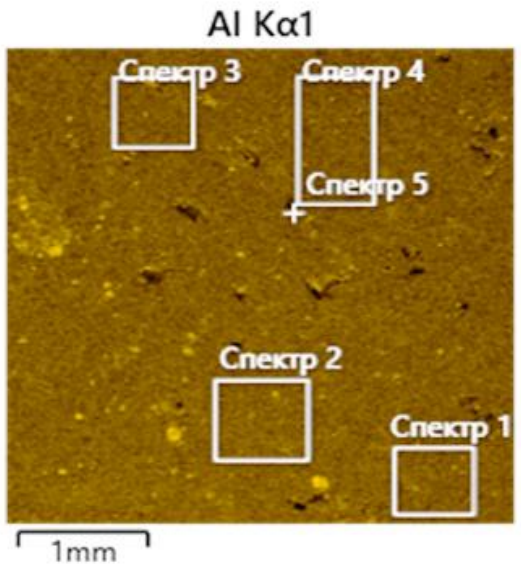

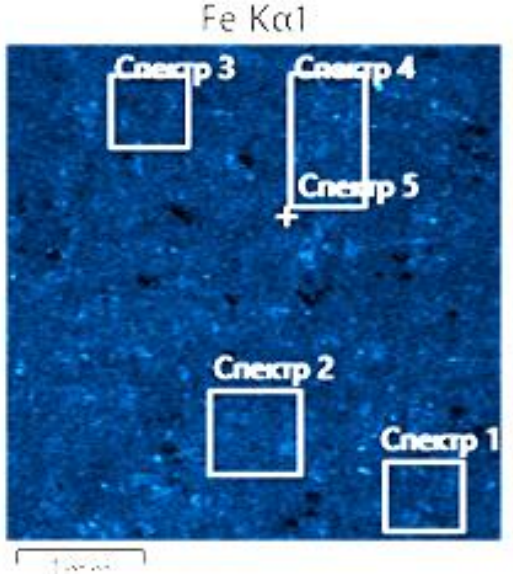

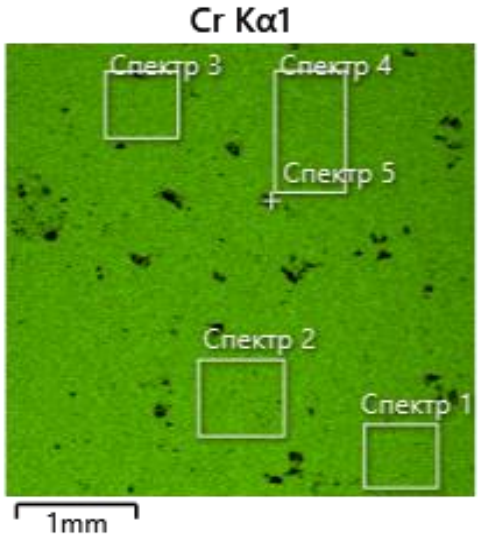

pores

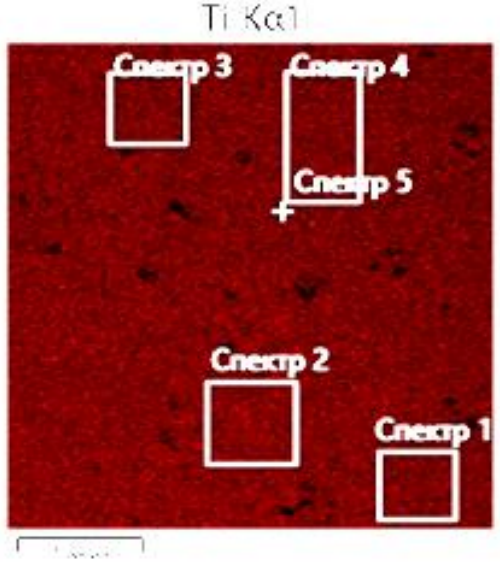

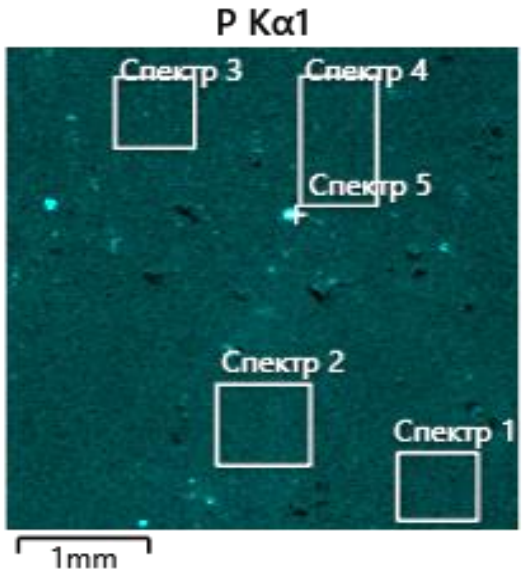

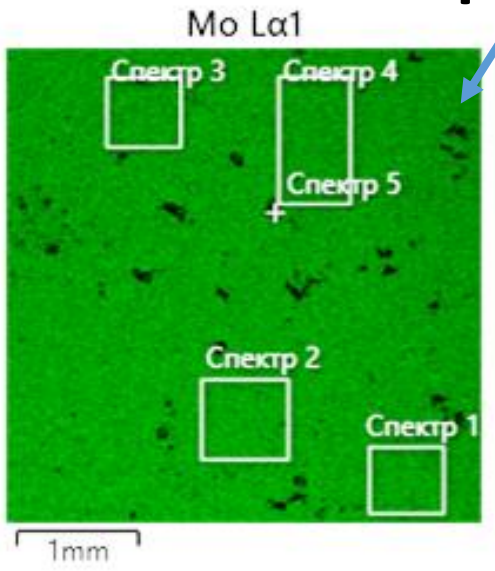

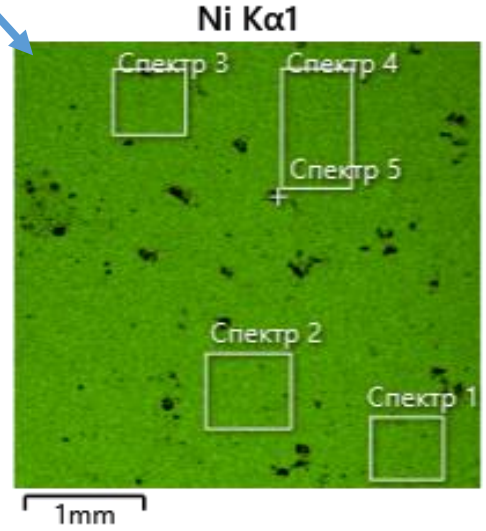

Structure of the alloy sample, as-build state, TEM

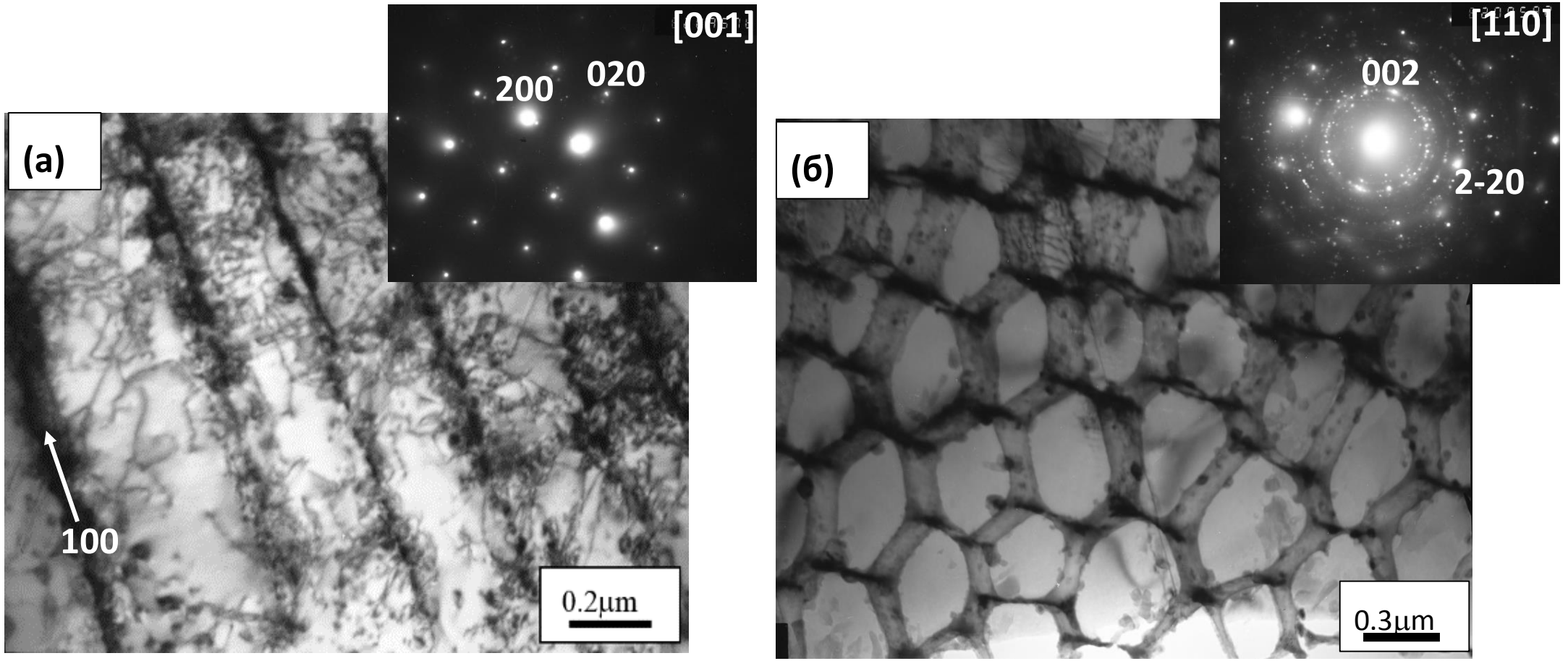

Cellular-dendritic structure of SLM alloy with a high density of defects: (a) –longitudinal section; (b) cross section

Structure of the alloy sample, as-build state, TEM

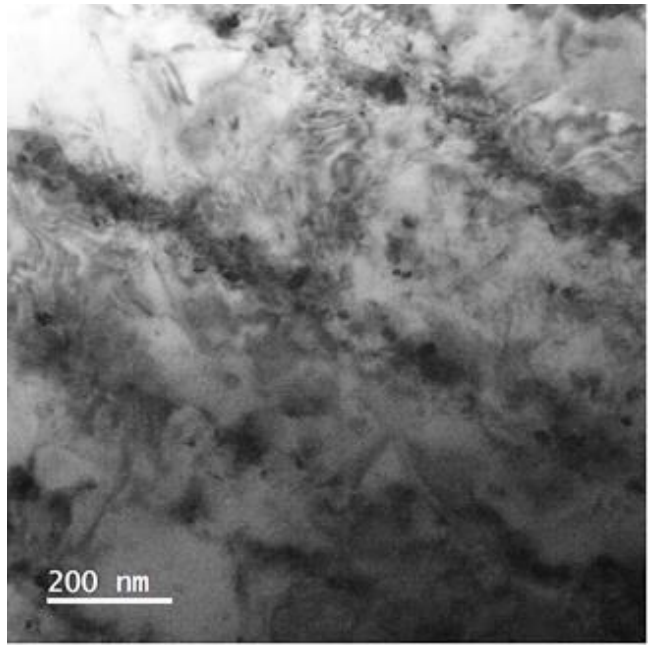

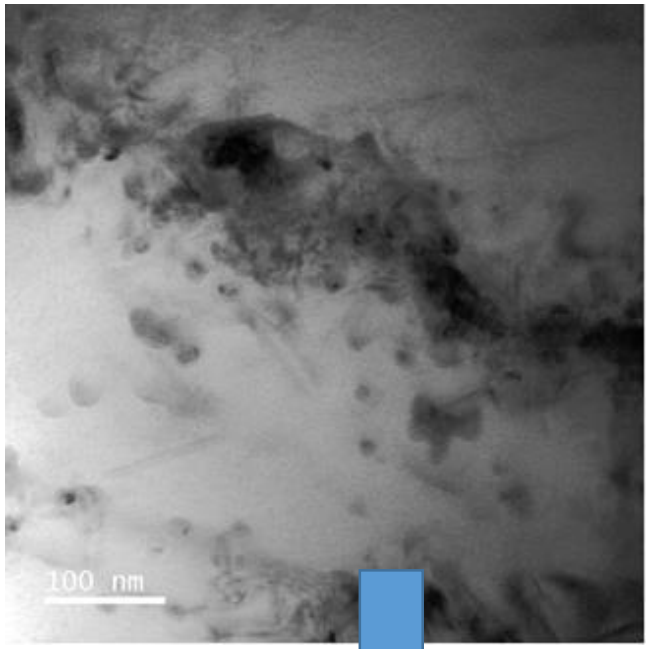

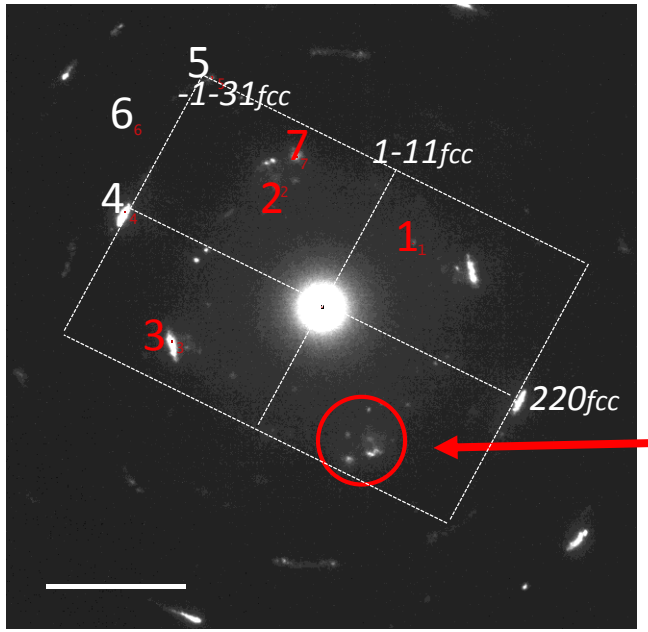

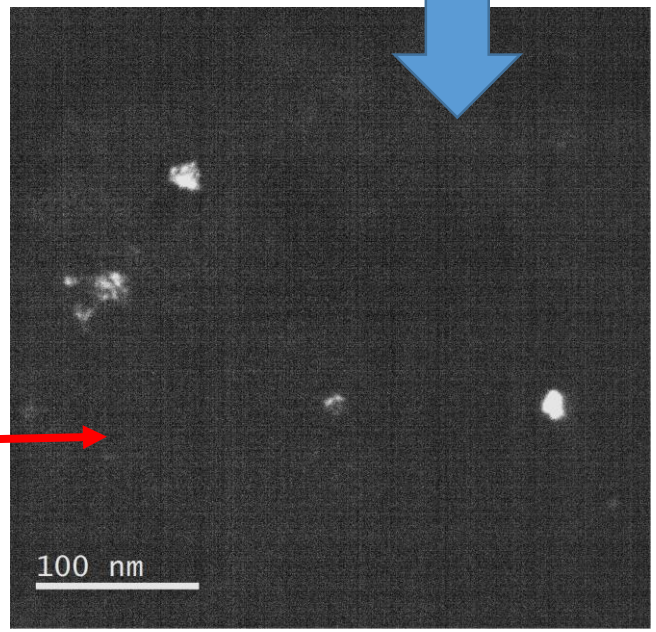

Spot, N	d-spacing, nm	
1	0.2500	→ 331 Me23C6
2	0.2145	→ 422 Me23C6
3	0.1816	→ 333 Me23C6
4	0.1276	→ 220 fcc
5	0.1091	→ 311 fcc
6	0.1046	→ 222 fcc
7	0.1821	→ 442 Me23C6

[1-10]Me23C6 // [-112]fcc

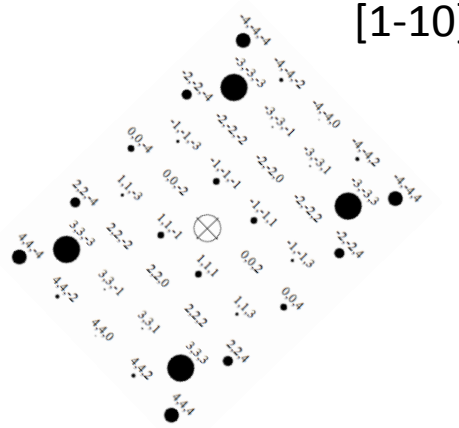

Structure of the alloy sample after aging 800C-15ч, TEM

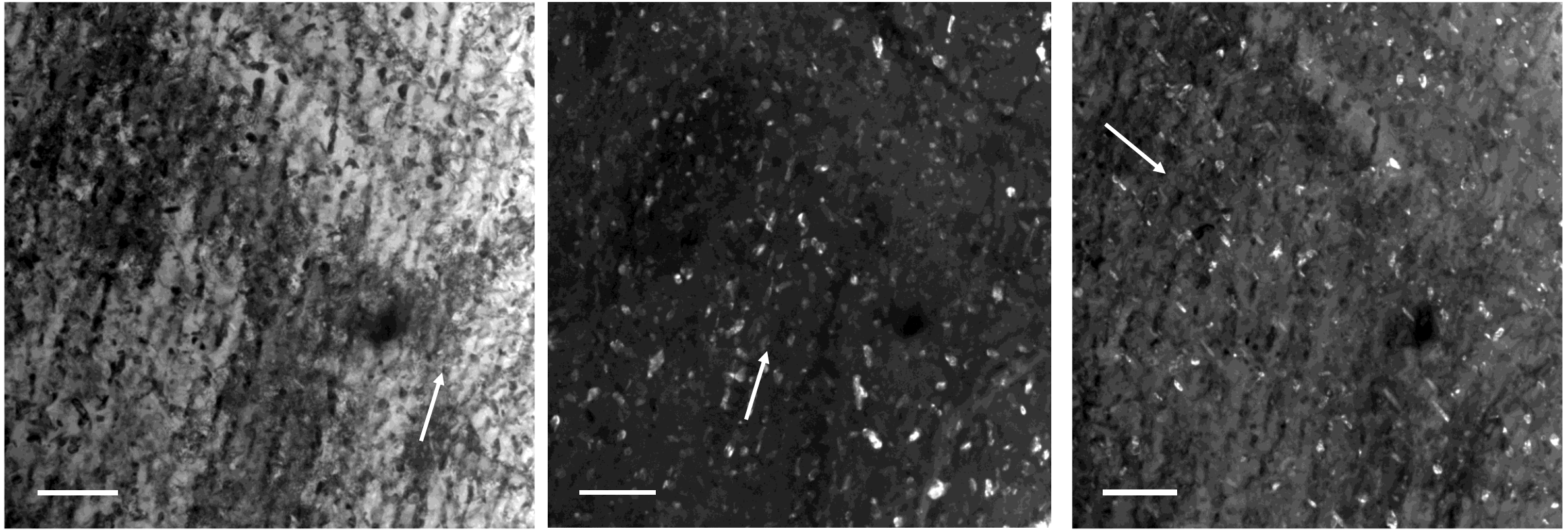

Structure of the alloy sample after aging 800C-15ч, TEM

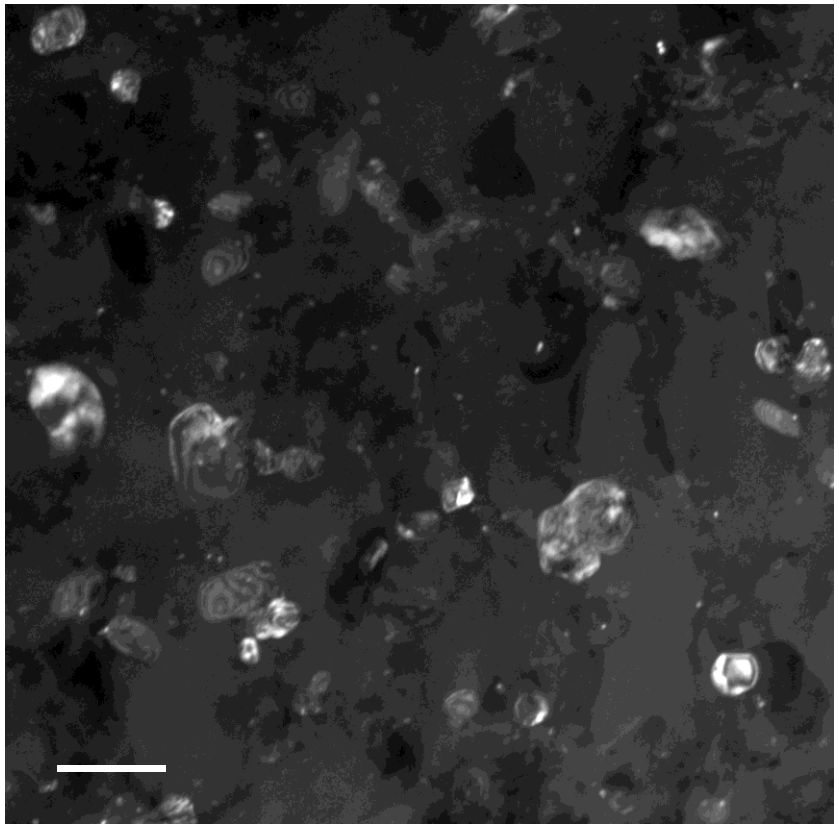

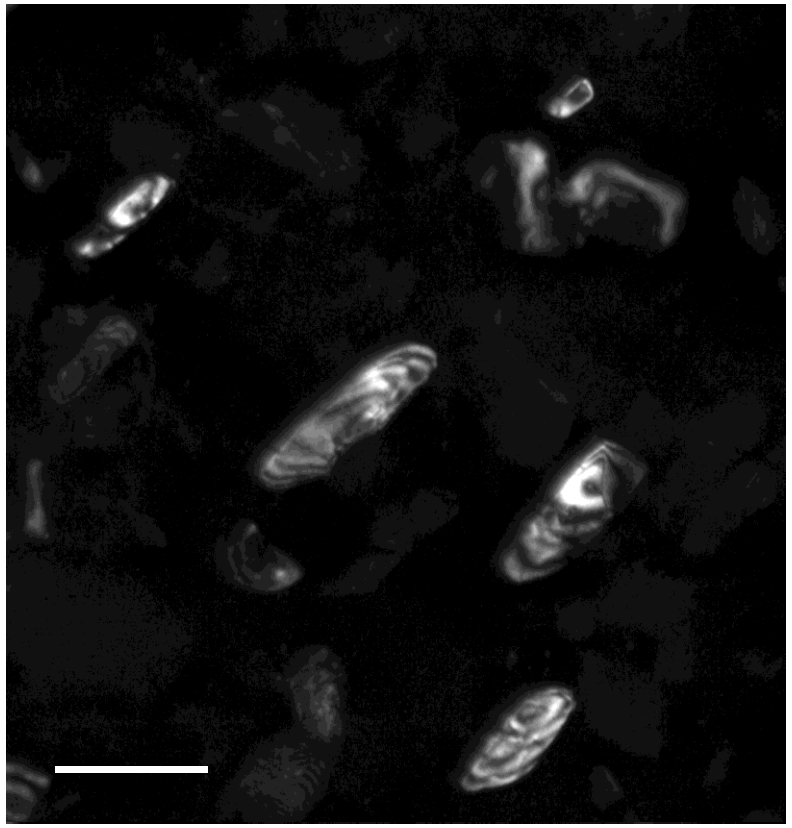

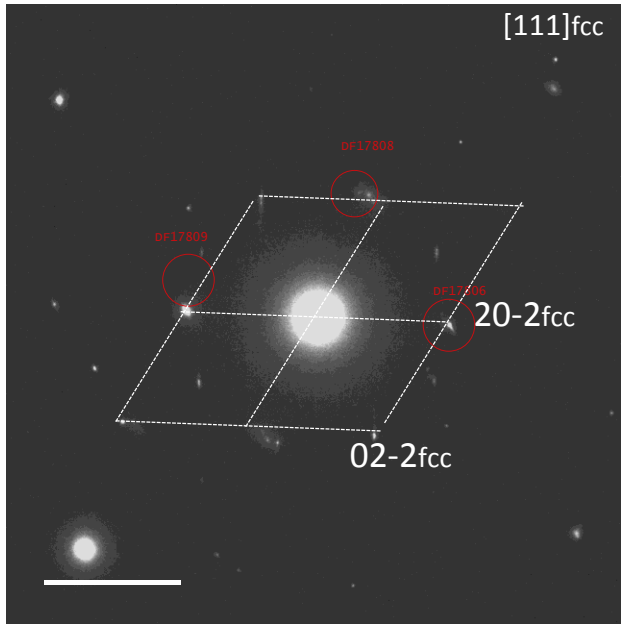

Carbide Me23C6 and σ-phase precipitations

Structure of the alloy sample after aging 800C-15ч, TEM

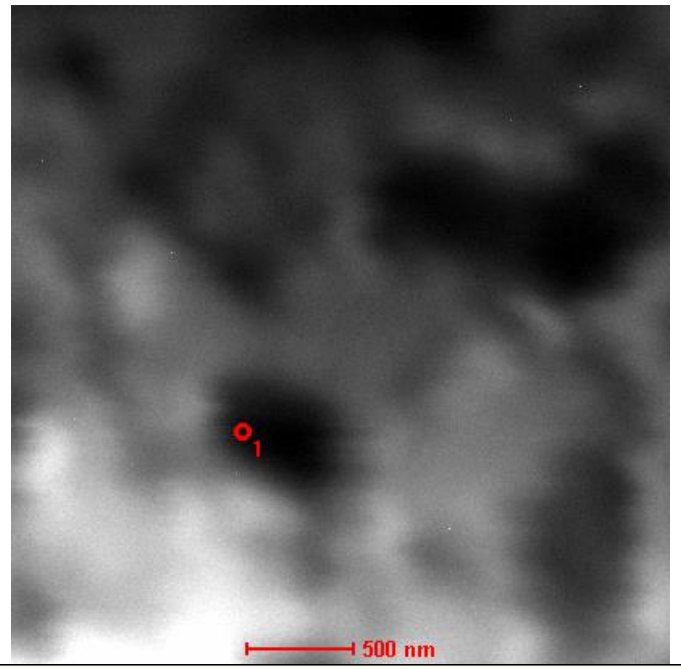

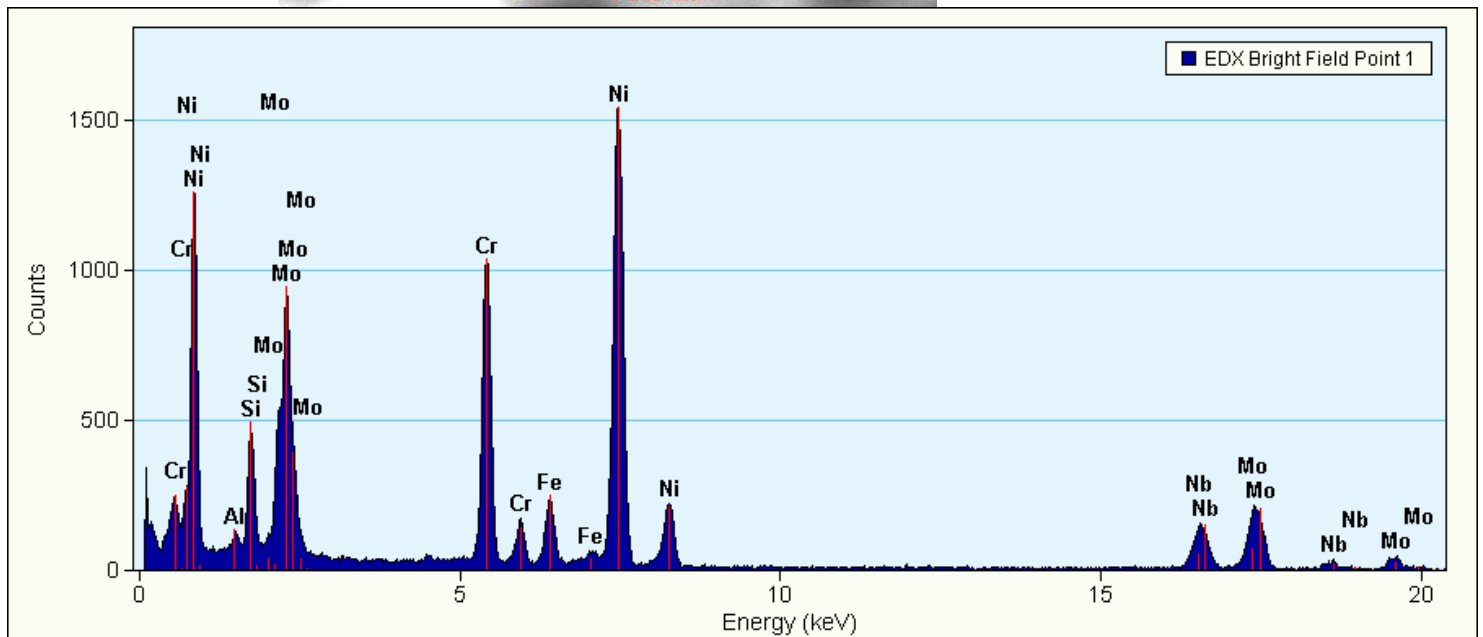

Element	Wt.%	at.%	
Al	1.2	2.8	2.0
Si	4.6	10.1	0.8
Cr	18.8	22.3	28.7
Fe	4.6	5.0	2.8
Ni	35.2	36.7	55.8
Nb	13.9	9.2	2.7
Mo	21.7	13.9	6.3

σ- $(Ni, Nb, Fe)_{0.51}(Cr,Mo, Al,Si)_{0.49}$,
type $Cr_{0,49}Fe_{0,51}$,
space group $P4_2 / mnm$, 136

Structure of the alloy sample after aging 800C-15ч, TEM

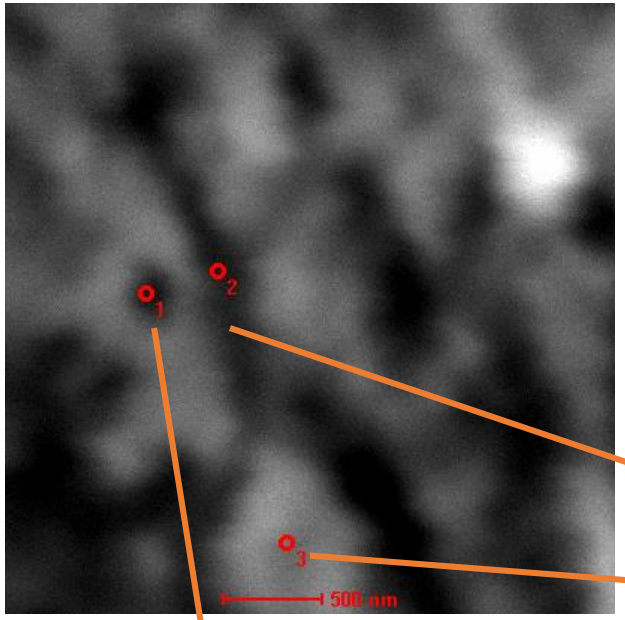

Me23C6?

O1

Element	Wt.%	at.%
Al	4.2	8.6
Si	1.8	3.7
Cr	23.2	24.7
Fe	4.9	4.9
Ni	54.7	51.5
Nb	4.5	2.7
Mo	6.7	3.9

2.0
0.8
28.7
2.8
56
3.4
6.3

O2

Element	Wt.%	at.%
Al	3.5	7.2
Si	0.9	1.8
Cr	27.2	28.8
Fe	7.5	7.4
Ni	49.3	50.7
Nb	2.6	1.5
Mo	4.5	2.6

O3

Element	Wt.%	at.%
Al	3.5	7.2
Si	1.2	2.4
Cr	24.7	26.2
Fe	6.9	6.8
Ni	57	53.5
Nb	2.2	1.3
Mo	4.5	2.6

$$Cr \xrightarrow{15-20\%\ [C]} Cr_{23}C_6 \xrightarrow{20-30\%\ [C]} Cr_7C_3 \xrightarrow{30-45\%\ [C]} Cr_3C_2$$

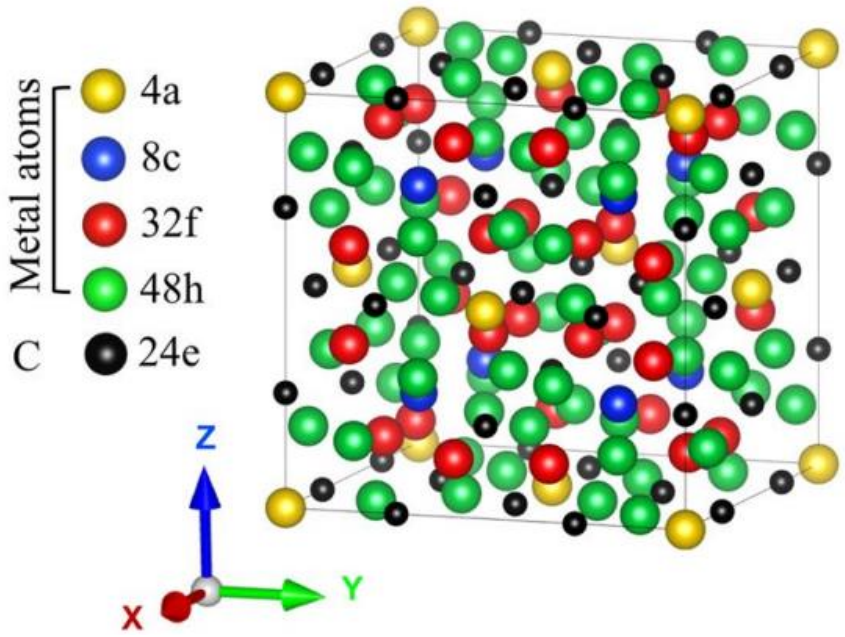

The γ-$Cr_{23}C_6$ (a=1.524 nm) supercell consists of one conventional unit cells with four inequivalent metal sites, namely, the 4a, 8c, 32f, and 48h sites, according to Wyckof notation. The C atoms are located at the 24e sites. Carbon vacancy formation enthalpy is very large [1]. In depending on the chemical content, the alloying elements may occupy different vacancies in the Cr sublattice. For example, Fe is found to preferentially substitute for Cr at the 4a site. When the iron content increases, Fe uptake in the 32f and 48h sites [1].

- In our case, a deviation from the stoichiometric composition of the γ-Cr23C6 carbide and the appearance of a large number of vacancies in the chromium sublattice may be associated with a high cooling rate of the material in the 3D laser printing method.

$A_{23-x}B_xC_6$, $M_{23}C_6$ (M = Cr, Fe), Fe in γ- $Cr_{23-x}Fe_xC_6$ in the range of $0 \le x \le 7.36$ wt.%.
$M_{23}C_6$-type carbides in multicomponent alloys may contain more than one metallic element $M_{23}C_6$(M = V, Cr, Mn, Fe, Co, Ni) [2].

[1] *Souissi, M., et al., Effect of mixed partial occupation of metal sites on the phase stability of γ-$Cr_{23-x}Fe_xC_6$ (x = 0–3) carbides. Scientific Reports, 2018. 8(1): p. 7279.*
[2] *N.I. Medvedeva et al. Stability of binary and ternary M23C6 carbides from first principles. Computational Materials Science 96 (2015) 159–164.*

- **The γ′ phase** precipitations were detected after heat treatment of the L-PBF KHN58MBYU alloy HIP+ 800C-500h in [1]. The size of the γ′-phase particles was 50 nm.
- The multicomponent **carbide (Cr, Mo)$_{23}$C$_6$** with sizes from 200 nm to 1 micrometer were observed to be formed along the boundaries of the cell-dendritic structure and at the grain boundaries [1].
- Also, the thin plate-like precipitations, suggested as **carboborides** [2] or **σ-phase** [3], were observed in L-PBF KHN58MBYU alloy after heat treatments HIP+ 800C-500h.

[1] *С. М. Прагер, Т. В. Солодова, О. Ю. Татаренко. ИССЛЕДОВАНИЕ МЕХАНИЧЕСКИХ СВОЙСТВ И СТРУКТУРЫ ОБРАЗЦОВ, ПОЛУЧЕННЫХ МЕТОДОМ СЕЛЕКТИВНОГО ЛАЗЕРНОГО СПЛАВЛЕНИЯ (СЛС) ИЗ СПЛАВА ВЖ159. Труды ВИАМ, №11, 2017.*
[2] *И.С. Мазалов, А.Г. Евгенов, С.М. Прагер. Перспективы применения жаропрочного структурно стабильного сплава ВЖ159 для аддитивного производства высокотемпературных деталей ГТД. Авиационные материалы и технологии. № S1(43). 2016*
[3] *Е.Н. Каблов, А.Г. Евгенов, И.С. Мазалов, С.В. Шуртаков, Д.В. Зайцев, С.М. Прагер. ЭВОЛЮЦИЯ СТРУКТУРЫ И СВОЙСТВ ВЫСОКОХРОМИСТОГО ЖАРОПРОЧНОГО СПЛАВА ВЖ159, ПОЛУЧЕННОГО МЕТОДОМ СЕЛЕКТИВНОГО ЛАЗЕРНОГО СПЛАВЛЕНИЯ. Ч. I Материаловедение. №3, С.9-17. 2019.*

CONCLUSION

1. The defects and features of the formation of equilibrium and nonequilibrium structures during 3D laser printing and subsequent heat treatment of heat-resistant nickel alloy KHN58MBYU used for the manufacture of gas turbine engine parts are investigated.
2. It was found that a cellular-dendritic structure with a high density of dislocations inside the cells is formed in the alloy after 3D laser printing.
3. Nanoscale (20 nm) separations of complex chromium carbide $(Cr,M)_{23}C_6$, M=Fe were found at the cell boundaries.
4. After annealing 800C-15 hours, the amount of complex chromium carbide $(Cr,Fe)_{23}C_6$ increases. The particles are shaped like disks, 50 nm thick and 200 nm in diameter.In addition to the complex carbide $(Cr,Fe)_{23}C_6$, particles of TCP sigma phase $(Ni, Nb, Fe)_{0.51}(Cr, Mo, Al, Si)_{0.49}$ were found in the alloy after annealing.
5. The precipitations of the intermetallic compound Ni_3Al were not found.